Aerosolized Ebola vaccine protects primates and elicits lung-resident T cell responses

Michelle Meyer,[1,2,3] Tania Garron,[1,2,3,4] Ndongala M. Lubaki,[1,2,3] Chad E. Mire,[2,3,4] Karla A. Fenton,[2,3,4] Curtis Klages,[2,3,5] Gene G. Olinger,[6] Thomas W. Geisbert,[2,3,4] Peter L. Collins,[7] and Alexander Bukreyev[1,2,3,4,8]

[1]Department of Pathology, [2]Galveston National Laboratory, [3]The University of Texas Medical Branch, [4]Department of Microbiology and Immunology, and [5]Animal Resources Center, Galveston, Texas, USA. [6]Viral Pathogenesis and Immunology Branch, Virology Division, United States Army Institute for Infectious Diseases, Frederick, Maryland, USA. [7]RNA Viruses Section, Laboratory of Infectious Diseases, National Institute of Allergy and Infectious Diseases, NIH, Bethesda, Maryland, USA. [8]Sealy Center for Vaccine Development, Galveston, Texas, USA.

Direct delivery of aerosolized vaccines to the respiratory mucosa elicits both systemic and mucosal responses. This vaccine strategy has not been tested for Ebola virus (EBOV) or other hemorrhagic fever viruses. Here, we examined the immunogenicity and protective efficacy of an aerosolized human parainfluenza virus type 3–vectored vaccine that expresses the glycoprotein (GP) of EBOV (HPIV3/EboGP) delivered to the respiratory tract. Rhesus macaques were vaccinated with aerosolized HPIV3/EboGP, liquid HPIV3/EboGP, or an unrelated, intramuscular, Venezuelan equine encephalitis replicon vaccine expressing EBOV GP. Serum and mucosal samples from aerosolized HPIV3/EboGP recipients exhibited high EBOV-specific IgG, IgA, and neutralizing antibody titers, which exceeded or equaled titers observed in liquid recipients. The HPIV3/EboGP vaccine induced an EBOV-specific cellular response that was greatest in the lungs and yielded polyfunctional $CD8^+$ T cells, including a subset that expressed CD103 (αE integrin), and $CD4^+$ T helper cells that were predominately type 1. The magnitude of the $CD4^+$ T cell response was greater in aerosol vaccinees. The HPIV3/EboGP vaccine produced a more robust cell-mediated and humoral immune response than the systemic replicon vaccine. Moreover, 1 aerosol HPIV3/EboGP dose conferred 100% protection to macaques exposed to EBOV. Aerosol vaccination represents a useful and feasible vaccination mode that can be implemented with ease in a filovirus disease outbreak situation.

Introduction

Ebola virus (EBOV) is a member of the family *Filoviridae*, which causes in humans and nonhuman primates (NHPs) the most severe hemorrhagic fever known, with a case fatality rate in most human outbreaks ranging from 47% to 88% (1, 2) and in NHPs close to 100% (3). Studies with NHPs suggest that aerosols of most biothreat agents, such as EBOV, are infectious (4) and that the virus can be transmitted though biological fluid droplets (5), fomites, and self-inoculation through contact (6). A recent study utilizing the guinea pig model demonstrated that contact with EBOV through mucosal surfaces of the respiratory tract results in respiratory infection (7). These observations suggest that respiratory tract mucosa may be an important portal of entry for EBOV, although more studies are required to clarify the issue (8), and emphasize the importance of immune protection of the respiratory tract. A noninvasive needle-free respiratory tract vaccine against EBOV therefore presents certain advantages. Immunization will not require trained medical personnel, making it particularly useful in areas of Africa that lack adequate infrastructure, where most EBOV disease outbreaks occur. Immunization or infection via the respiratory tract results in antigen presentation by mucosal respiratory dendritic cells, phenotypically and functionally distinct from those found in the spleen (9, 10), to antigen-specific T lymphocytes localized in the respiratory tract, which are not significantly released into circulation (11, 12). These lung-resident T cells are phenotypically different and are more activated in response to respiratory viruses than their peripheral blood counterparts specific for the same virus (11), thus providing additional protection against infection through the respiratory tract.

Previous preclinical studies by ourselves (13) and others (14) have demonstrated that mucosal respiratory tract vaccination efficiently induces both mucosal and systemic immune responses. The only approved respiratory vaccine in the US is FluMist (15). Studies on the induction of the mucosal immune responses in the lung in convenient experimental animals such as the mouse are not necessarily predictive for humans due to fundamental differences in immune regulation (16, 17). Therefore, it is essential to focus on humans or NHPs. The mucosal cell–mediated responses to respiratory tract vaccinations or viral infections can only be reliably evaluated by ex vivo analysis of lymphocytes isolated from the lung tissue (11) and remain poorly characterized. To our knowledge, only one study utilized human lung biopsy material to demonstrate that the relative enrichment of differentiated influenza A– and respiratory syncytial virus–specific memory $CD8^+$ T lymphocytes in human lung tissues exceeded that in the peripheral blood by as much as 20- and 15-fold, respectively (11).

Previously, we developed a human parainfluenza virus type 3–based replication-competent vaccine (HPIV3/EboGP) that expresses the envelope glycoprotein (GP) of EBOV, isolate Mayinga (GenBank AAG40168.1) (18). The GP protein was packaged

Conflict of interest: The authors have declared that no conflict of interest exists.
Submitted: February 17, 2015; **Accepted:** May 28, 2015.
Reference information: *J Clin Invest*. 2015;125(8):3241–3255. doi:10.1172/JCI81532.

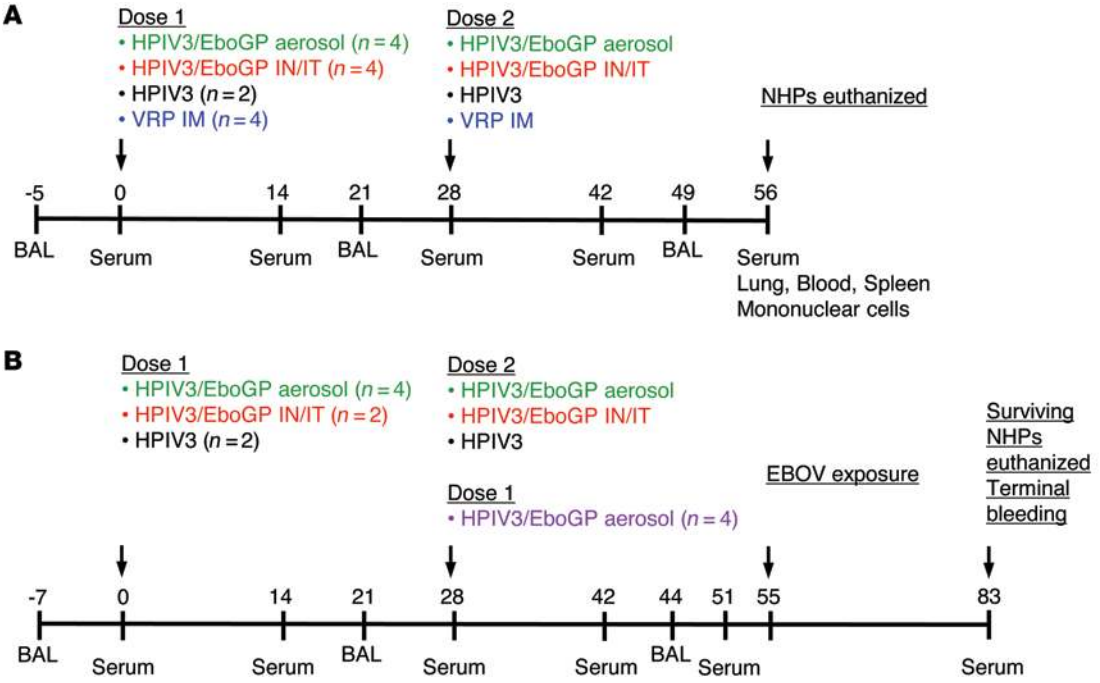

Figure 1. Schedules of vaccinations, biosamplings, and EBOV exposure. (**A**) Study 1: NHP immune response to vaccination. Groups of rhesus macaques were vaccinated with HPIV3/EboGP as an aerosol (n = 4; green) or a liquid via the i.n./i.t. (n = 4; red) route, the empty HPIV3 vector control (n = 2; black), or the VRP vaccine by the i.m. route (n = 4; blue). Twenty-eight days after the first dose, all NHPs received a second dose of their respective vaccine. On day 56, NHPs were euthanized and mononuclear cells were extracted. (**B**) Study 2: testing of protective efficacy. Groups of rhesus macaques were vaccinated with 1 (n = 4; purple) or 2 doses (n = 4; green) of aerosolized HPIV3/EboGP, 2 doses of liquid HPIV3/EboGP (n = 2; red), or HPIV3 control (n = 2; black). Fifty-five days after vaccination, NHPs were infected with EBOV. At the end of the study, surviving animals were euthanized and terminal bleed samples were collected. Over the course of the 2 studies, serum and BAL samples were collected on indicated days.

into the vector particle and was functional in mediating infection of the respiratory tract, but did not alter the tropism of the vaccine virus (18–20). Rhesus macaques were protected against a lethal dose of EBOV when 2 successive liquid doses of the vaccine were administered using the combined intranasal and intratracheal (i.n./i.t.) instillation procedure (21). Meanwhile, aerosolized delivery has never been tested for our vaccine or any other viral hemorrhagic fever vaccine. Vaccine aerosolization through the use of portable, disposable nebulizers may be the most practical, convenient, and effective way to use our mucosal vaccine, enabling delivery to the lower respiratory tract. Lung-resident $CD8^+$ T lymphocytes may be of paramount importance for protection against EBOV transmission via the respiratory mucosa, as in the case of natural outbreaks, or if used as an aerosolized weapon for bioterrorism and biological warfare (22), and $CD4^+$ T lymphocytes in lung tissues are important for activation of systemic and mucosal antibody responses. Other EBOV vector–based vaccine systems demonstrate that both cellular and humoral immunity may contribute to protection against EBOV infection (23, 24). Our previous study primarily quantified local and systemic antibody responses. The lung-resident T lymphocyte response induced by our respiratory tract vaccine and the balance between mucosal and systemic responses have not been previously analyzed.

The present study comprehensively characterizes the systemic and mucosal immune responses generated by vaccination with HPIV3/EboGP delivered to the respiratory tract as an aerosol or liquid. Direct comparisons were made with the protective, nonreplicative intramuscular (i.m.) Venezuelan equine encephalitis virus replicon particle (VRP) vaccine expressing EBOV GP (25). This included comparisons between tissue-resident T cell responses in the lungs and spleen and peripheral blood T cells. A single vaccination with aerosol HPIV3/EboGP was sufficient to protect rhesus macaques against the death and severe disease caused by lethal EBOV infection.

Results

Study 1

Systemic and mucosal antibody– and cell-mediated responses to aerosol vaccination. Study 1 was designed to compare the EBOV-specific mucosal and systemic antibody and cell-mediated responses in rhesus macaques induced by respiratory tract vaccination with HPIV3/EboGP delivered as an aerosol or as a liquid or i.m. delivery of VRP expressing EBOV GP (ref. 25 and Figure 1A). Groups of rhesus macaques received 2 doses of HPIV3/EboGP or the control empty HPIV3 vector (wild-type virus) by i.n./i.t. delivery at $10^{7.3}$ PFU per site in the form of a liquid. While aerosol particles less than 3 μM in diameter readily penetrate the small airways (26), the recipients of aerosolized HPIV3/EboGP received a 10-fold higher dose of the vaccine to account for a 10% delivery efficiency of aerosol particles to the lower respiratory tract in primate models due to small lung size and shallow breathing patterns (27, 28) further exacerbated by anesthesia during vaccination (26). The VRP group was vaccinated by 2 sequential s.c. injections of 10^{10} infec-

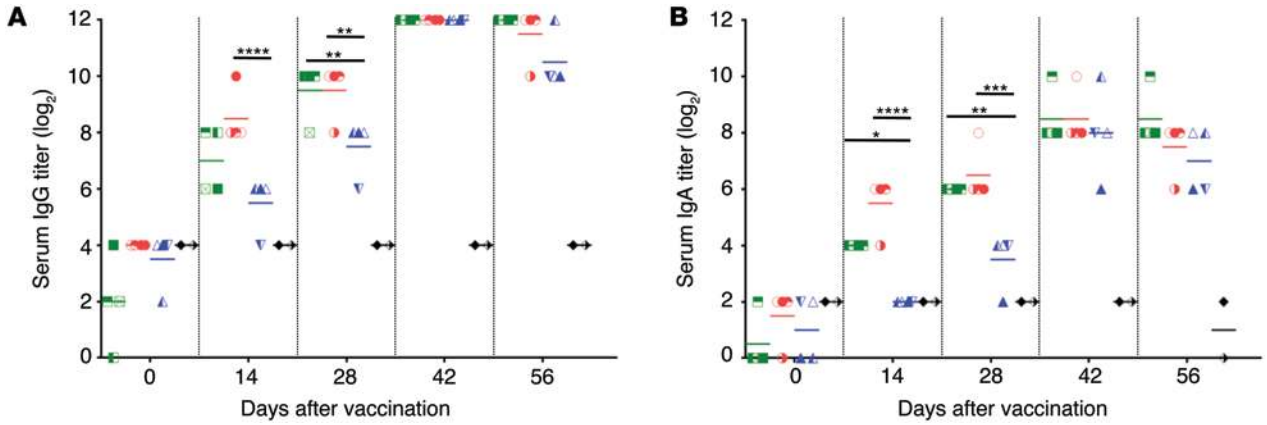

Figure 2. Serum IgG and IgA response in NHPs from vaccination study 1. NHPs received 2 doses of aerosolized (n = 4; green) or liquid (n = 4; red) HPIV3/EboGP, VRP vaccine (n = 4; blue), or the HPIV3 control (n = 2; black). EBOV-specific serum (**A**) IgG and (**B**) IgA were analyzed by ELISA. Values are shown for individual animals in each vaccine group with horizontal bars representing group means. *P < 0.05; **P < 0.01; ***P < 0.001; ****P < 0.0001, by 2-way ANOVA with Tukey's post-hoc test. For clarity, comparisons to VRP on days 14 and 28 are shown.

tious units of the construct, the optimal regimen protective against EBOV exposure in cynomolgus macaques (ref. 29, G.G. Olinger, unpublished observations); in recent studies, accelerated protection of cynomolgus macaques after a single dose was achieved (30). To analyze the systemic and mucosal antibody responses, we collected the serum separated from peripheral blood and bronchoalveolar lavages (BAL), respectively, from all animals, with the exception of BAL from those in the VRP vaccine group, which were not expected to develop a respiratory mucosal antibody response. Animals were euthanized on day 56, and mononuclear cells were isolated from the lung and spleen tissues and blood to determine response differences from lung-residing T cells versus T cells from the periphery based on route of vaccination and type of vaccine.

Aerosol vaccination induces the robust systemic antibody responses. Analysis of antibody responses by ELISA demonstrated detectable titers of EBOV-specific IgG and IgA in animals vaccinated with HPIV3/EboGP in a liquid or aerosolized form starting at day 14 after vaccination, with a small increase by day 28 (Figure 2, A and B). Administration of the second dose, on day 28, resulted in a strong increase in antibody levels by day 42. Compared with HPIV3/EboGP vaccination, VRP induced lower levels of IgG and IgA on day 14. However, titers reached parity following the second dose.

Surface plasmon resonance (SPR) analysis of total EBOV-binding antibody (Supplemental Figure 1, A and B; supplemental material available online with this article; doi:10.1172/JCI81532DS1) revealed a robust response in HPIV3/EboGP-vaccinated animals after dose 1 (day 28), which slightly increased after dose 2 (day 56) to yield somewhat higher levels in aerosol recipients. Compared with HPIV3/EboGP recipients, VRP-vaccinated animals exhibited weaker EBOV antibody–binding profiles; 3-fold fewer EBOV-binding antibodies were generated after dose 1, but numbers rose after dose 2 so that they were marginally lower than levels in HPIV3/EboGP recipients. Antibody avidity was determined by analysis of antibody dissociation rates (off-rate), where a low value was indicative of higher avidity (Supplemental Figure 1C). After dose 1, the dissociation rates of antibodies from aerosol and liquid HPIV3/EboGP-vaccinated animals were equal and lower than those of VRP-vaccinated animals, suggesting that higher avidity antibodies were generated by the respiratory vaccine. The VRP group displayed a more heterogeneous antibody off-rate profile. The second vaccine dose did not alter the dissociation rates of antibodies from HPIV3/EboGP-vaccinated animals. In contrast, the dissociation rate of antibodies from each VRP-vaccinated animal was reduced, with 3 out of 4 animals exhibiting rates equal to those observed in HPIV3/EboGP-vaccinated animals.

Testing of the ability of sera to neutralize EBOV in vitro demonstrated comparable neutralizing titers in animals vaccinated with either forms of HPIV3/EboGP, which reached high levels after dose 1 (mean titers 1:460 and 1:250 for aerosolized and liquid forms, respectively) and were only slightly increased after dose 2 (Figure 3A). Following vaccination with VRP, neutralizing titers were low after dose 1, but increased to levels comparable to those in HPIV3/EboGP-vaccinated animals after dose 2. Taken together, these data suggest that vaccination with aerosolized HPIV3/EboGP induces systemic antibody responses comparable to those after respiratory vaccination with liquid HPIV3/EboGP. The data also show that following dose 1, the antibody response to HPIV3/EboGP was greater in magnitude and avidity than that to VRP.

Two vaccine doses induce neutralizing antibodies against heterologous EBOVs. The breadth of the antibody response was determined by the ability to cross-neutralize EBOVs Bundibugyo (BDBV) and Sudan (SUDV). Following dose 1, only 1 HPIV3/EboGP liquid and 1 VRP recipient demonstrated detectable BDBV-neutralizing titers of 1:33 and 1:15, respectively. However, after dose 2, comparable titers were achieved in most animals from all vaccine groups (Figure 3B). In contrast to BDBV, SUDV-neutralizing antibodies were detected in most animals after dose 1 and in all animals except 2 liquid HPIV3/EboGP recipients after dose 2 (Figure 3C). Compared with the HPIV3/EboGP vaccine, 2 doses of VRP yielded markedly higher BDBV- and SUDV-neutralizing titers. Taken together, these data suggest that antibody cross-neutralization is stronger following administration of 2 vaccine doses and that the breadth of the response has considerable animal-to-animal variability.

Respiratory vaccination induces mucosal antibodies in the respiratory tract. To analyze mucosal antibody responses in the respiratory tract, concentrated BAL collected from animals vaccinated

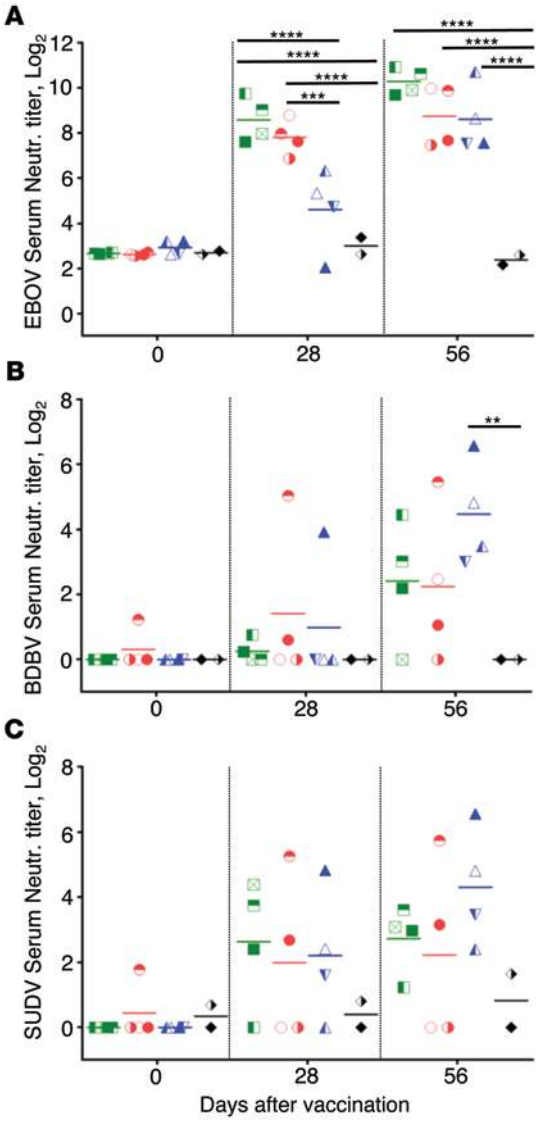

Figure 3. Serum-neutralizing antibody responses in NHPs from vaccination study 1. NHPs received 2 doses of aerosolized (n = 4; green) or liquid (n = 4; red) HPIV3/EboGP, VRP vaccine (n = 4; blue), or the HPIV3 control (n = 2; black). Serum-neutralizing antibody responses against (**A**) EBOV, (**B**) BDBV, and (**C**) SUDV were determined by plaque-reduction assays. Values are shown for individual animals in each vaccine group, with horizontal bars representing group means. $^{**}P < 0.01$; $^{***}P < 0.001$; $^{****}P < 0.0001$, by 2-way ANOVA with Tukey's post-hoc test.

with either forms of HPIV3/EboGP or the empty HPIV3 vector were analyzed by ELISA and virus neutralization assays. High titers of IgG and IgA were detected in aerosol and liquid HPIV3/EboGP recipients after dose 1, and titers further increased following dose 2 (Figure 4, A and B). The mean neutralizing antibody titers in aerosolized and liquid recipients reached 1:9 and 1:23, respectively, after dose 1 and 1:112 and 1:47 after dose 2 (Figure 4C). Thus, aerosol vaccination induces robust mucosal antibody responses in the respiratory tract.

Respiratory vaccination induces a more robust T cell response in the lungs than in blood and spleen. Mononuclear cells derived from tissues of the lungs, blood, and spleen were stimulated with peptides spanning the entire EBOV GP, and $CD8^+$ T cell subpopulations positive or negative for CD103, a marker highly expressed by mucosal $CD8^+$ T lymphocytes, and $CD4^+$ T cells, were analyzed for functional markers of activation by flow cytometry (Figure 5). The magnitude of both the $CD8^+$ and $CD4^+$ T cell response induced by HPIV3/EboGP was dramatically greater in the lungs than in the blood or spleen. For example, in aerosolized HPIV3/EboGP recipients, the mean percentages of lung $CD103^+CD8^+$ T cells secreting TNF-α were 15- and 28-fold greater than in the blood and spleen, respectively. The mean percentages of lung $CD4^+$ T cells secreting TNF-α were 12- and 14-fold greater than in blood and spleen, respectively. These data suggest the cell-mediated response occurs predominately in the respiratory tract, the site of HPIV3/EboGP replication, with limited, but detectable, systemic spread of these virus-specific lymphocytes.

The activated $CD8^+$ cells are almost equally divided between the $CD103^+$ and $CD103^-$ populations. CD103 is expressed at high levels by mucosal $CD8^+$ T cells, specifically those associated with lung tissue, and is involved with their mucosal homing, cytotoxicity against respiratory epithelial cells, and retention as effector memory T cells (31). We therefore compared distribution of the activated $CD103^+CD8^+$ T cells and their $CD103^-$ counterparts at 3 different sites. In lungs, the activated $CD8^+$ cells were almost equally distributed as $CD103^+$ and $CD103^-$ populations (Figure 6). Contrary to our expectations, the frequency of activated $CD103^-$ populations in the blood and spleen was only marginally higher than that of the $CD103^+CD8^+$ T cells (Figure 6). These data suggest that the $CD103^+$ fraction of activated $CD8^+$ T cells may be active not only at mucosal sites but also in the periphery.

Respiratory vaccination induces a greater activation of $CD8^+$ T cells in lungs than in blood and spleen. The majority of EBOV-specific lung-resident $CD8^+$ T cells induced by HPIV3/EboGP were polyfunctional, i.e., positive for 2 or more of the 4 markers of activation (CD107a, IFN-γ, IL-2, and TNF-α). Cells expressing all 4 markers of activation were rare, observed mainly in recipients of the liquid form of HPIV3/EboGP (Figure 6). $IFN\text{-}\gamma^+IL\text{-}2^+TNF\text{-}\alpha^+$ in the absence of CD107a dominated the triple-marker functional responses. The double-positive cell populations were generally characterized by cells producing IFN-γ in combination with TNF-α or IL-2. Small numbers of cells possessed an $IL\text{-}2^+TNF\text{-}\alpha^+$ phenotype, while combinations with CD107a were only elicited by 2 animals, which received the liquid HPIV3/EboGP vaccine. There was no clear association between the polyfunctional response pattern in the lungs versus the spleen and blood. Moreover, the proportion of the polyfunctional response was generally lower in the blood and spleen, with the majority of cells positive for only a single marker of activation and varying trends among the respiratory vaccinees (Figure 6). These data suggest that respiratory vaccination with HPIV3/EboGP not only induces a greater number of $CD8^+$ T cells in lungs than in blood and spleen, but also results in a greater activation of lung $CD8^+$ T cells.

Respiratory vaccination induces a greater activation of $CD4^+$ T cells in lungs and spleen than in blood. HPIV3/EboGP-activated $CD4^+$ T cells were analyzed for the production of any combination of IFN-γ, IL-4, IL-17, and TNF-α. At least 25% of cells in lungs

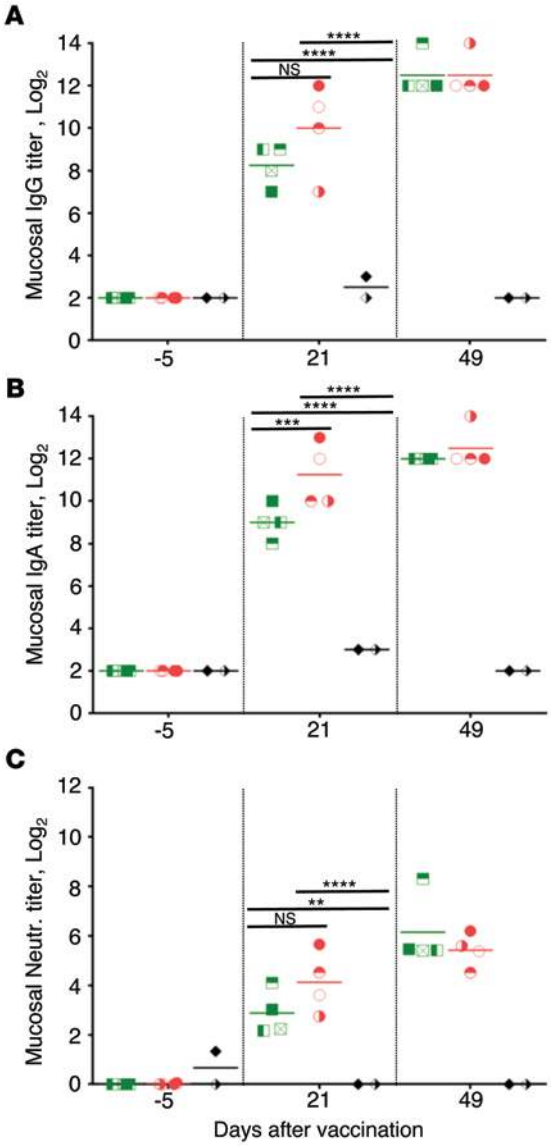

Figure 4. Mucosal antibody responses to HPIV3/EboGP in NHPs from vaccination study 1. NHPs received 2 doses of aerosolized (n = 4; green) or liquid (n = 4; red) HPIV3/EboGP or the HPIV3 control (n = 2; black). EBOV-specific (**A**) IgG and (**B**) IgA were determined by ELISA, and (**C**) EBOV-neutralizing antibodies were determined by a plaque-reduction assay. Values are shown for individual animals in each vaccine group, with horizontal bars representing group means. For clarity, comparisons on day 21 made with 2-way ANOVA with Tukey's post-hoc test are shown. $^{**}P < 0.01$; $^{***}P < 0.001$; $^{****}P < 0.0001$.

were positive for 2 markers of activation, namely TNF-α and IFN-γ (Figure 7). Other 2-functional response combinations were not detected. A strong monofunctional response pattern was also observed, dominated by the expression of TNF-α, a smaller fraction of IFN-γ$^+$ cells, and the absence of IL-4$^+$ cells. An analogous phenotypic pattern of activation markers was observed in the blood. However, bifunctional TNF-α$^+$IFN-γ$^+$ cells were detected at a much lower frequency, suggesting either a lower activation of CD4$^+$ T cells circulating in the blood or the retention of resident CD4$^+$ T cells in the lung serving as protectors against respiratory infections (Figure 7). Interestingly, the number of activated CD4$^+$ T cell populations was greater in the spleen than in the blood and mostly composed of either bifunctional TNF-α$^+$IFN-γ$^+$ populations or monofunctional IFN-γ, TNF-α, or IL-17 CD4$^+$ T cells. However, the frequency of these functional populations varied greatly among individual animals from each group (Figure 7). Following peptide stimulation, the level of IL-4 expression was significantly less in CD4$^+$ T cells isolated from the spleens of aerosol vaccinees compared with the control and VRP recipients (Figure 5C and Figure 7). This may be an indication of HPIV3/EboGP ability to produce a predominantly Th1 response against infection, while IL-4 expression in control animals may represent a background or inadequate response to peptide stimulation. Taken together, these data suggest that respiratory vaccination with HPIV3/EboGP induces the most potent CD4$^+$ T cell response in lungs, followed by spleen, and a substantially lower response in the peripheral blood.

Vaccination induces Th17 cells mostly in spleen. The role of Th17 in protection against viral infections is not clear: while some studies demonstrated their role in protection (32, 33), others suggested no role (34) or even enhancement of viral infection (35). Development of Th17 cells was previously associated with pulmonary immune defense (36) or inflammation in chronic obstructive pulmonary disease and lung cancer (37). Modest amounts of GP-specific CD4$^+$ T cells positive for IL-17 were detected in spleens of some of the vaccinated animals irrespective of the vaccine type and were rare in the lungs and blood (Figures 5 and 7), with no IL-17–inclusive activation marker combinations dominant in any of the 3 sites. The majority of IL-17–positive cells from the spleen were monofunctional (Figure 7). Only a few animals, specifically from the VRP group, yielded very low percentages of cells positive for IL-17 in combination with IFN-γ and IL-4 or IFN-γ only. While IL-17$^+$IFN-γ$^+$ cells correspond to the previously established Th17/Th1 phenotype (38), we are unaware of any previous identification of Th17 cells secreting IL-4. The protective role of Th17 cells induced by EBOV vaccines requires additional studies.

Delivery of HPIV3/EboGP in aerosolized form increases the T cell response in lungs. We next compared lung CD8$^+$ and CD4$^+$ T cell responses to liquid and aerosol administration of HPIV3/EboGP. Strikingly, IFN-γ$^+$IL-2$^+$TNF-α$^+$ and IFN-γ$^+$TNF-α$^+$ CD8$^+$ T cells were above 0.1% in all 4 aerosolized HPIV3/EboGP recipients, but only in 2 out of 4 i.n./i.t.–vaccinated animals (Figure 6). More aerosol recipients yielded higher percentages of lung CD8$^+$ T cells bifunctional for IFN-γ$^+$IL-2$^+$ and CD103$^+$CD8$^+$ T cells monofunctional for IFN-γ or TNF-α than seen in liquid vacinees. Interestingly, functional response combinations incorporating CD107a were mostly evident in some of the liquid HPIV3/EboGP vaccine recipients: their lung CD103$^+$ or CD103$^-$CD8$^+$ T cells were capable of CD107a mobilization. This trend was observed in the blood and spleen of these liquid recipients, though fewer CD103$^+$ cells were mobilizing CD107a (Figures 5 and 6). Lung CD103$^-$CD8$^+$ T cells in aerosolized HPIV3/EboGP recipients expressed more TNF-α than those of the liquid recipients (Figure 5D) even though the total cell numbers were comparable between these groups (Figure 5A).

While the total amount of CD4$^+$ T cells producing IFN-γ or TNF-α and the levels at which they express these cytokines were generally comparable between aerosol and liquid HPIV3/EboGP

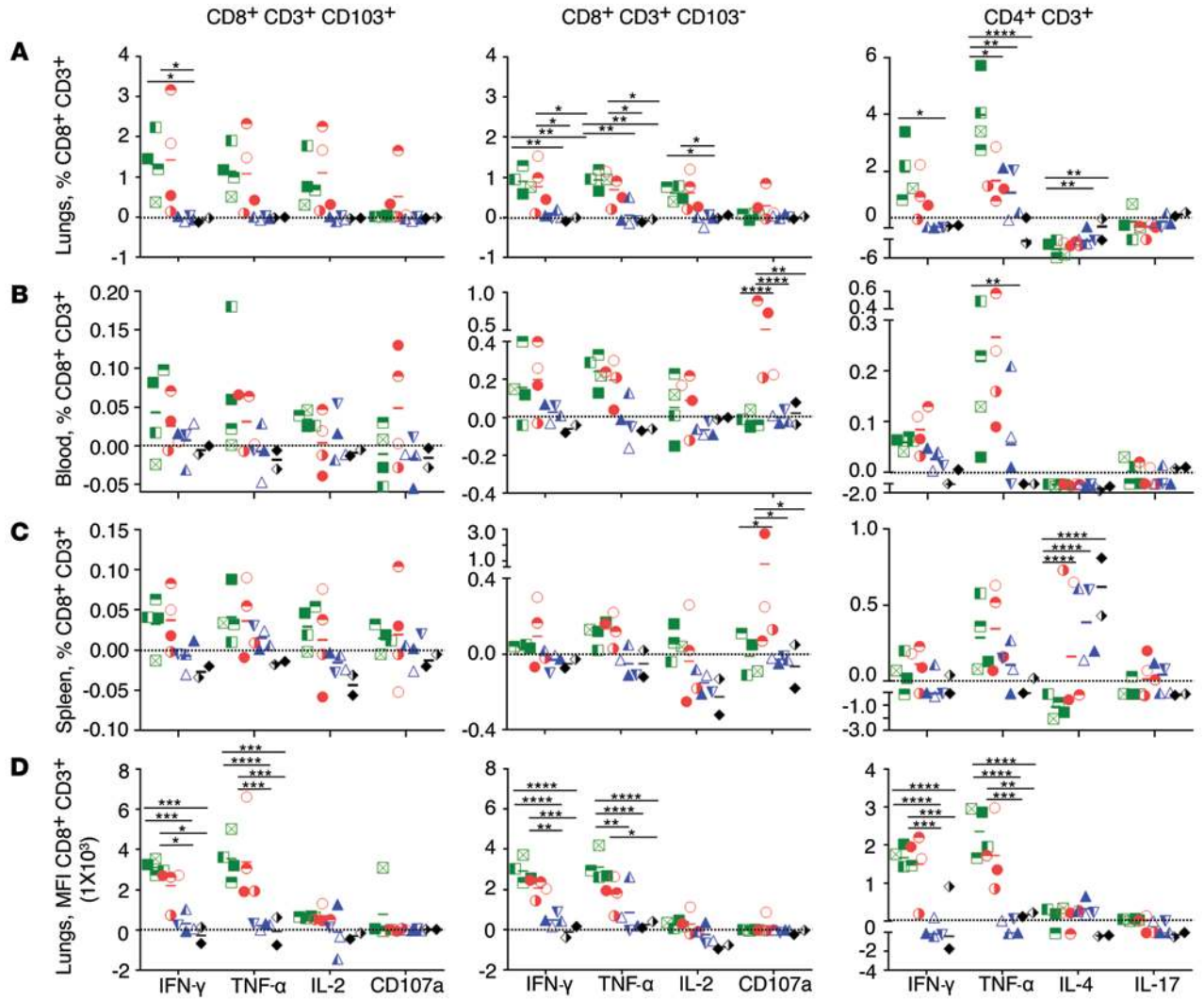

Figure 5. Cell-mediated response in vaccine recipients from study 1. NHPs were vaccinated with HPIV3/EboGP aerosol (n = 4; green symbols), HPIV3/EboGP liquid (n = 4; red), the VRP vaccine (n = 4; blue), or HPIV3 control (n = 2; black). Magnitude of $CD8^+$ $CD103^+$ (left) and $CD103^-$ (middle) T cell subsets and $CD4^+$ T cells (right) from the (**A** and **D**) lungs, (**B**) blood, and (**C**) spleen positive for markers of activation following GP peptide stimulation, displayed as (**A**–**C**) a percentage of total $CD8^+$ or $CD4^+$ cells or (**D**) level of expression (MFI). The group means are shown by horizontal bars. *P < 0.05; **P < 0.01; ***P < 0.001; ****P < 0.0001, by 2-way ANOVA with Tukey's post-hoc test.

recipients (Figure 5, A and D), the aerosol group had double the total number of lung $CD4^+$ T cells expressing TNF-α (Figure 5A). Analysis of multifunctional $CD4^+$ T cells demonstrated that bifunctional TNF-α^+IFN-γ^+ and monofunctional TNF-α^+ cells in lungs were 2.1- and 2.9-fold, respectively, greater in the aerosol HPIV3/EboGP group than in the liquid vaccine group (Figure 7). The greater activation of T cells in lungs by aerosolized HPIV3/EboGP may be the consequence of more efficient delivery to the pulmonary bronchiole and more efficient activation of pulmonary antigen-presenting cells, such as $CD103^+$ dendritic cells.

Vaccination with VRP induces T cells responses predominantly in spleen. Comparison of HPIV3/EboGP and VRP demonstrated that in both lungs and blood, greater numbers and proportions of polyfunctional $CD8^+$ and $CD4^+$ T cell populations were induced in most of the HPIV3/EboGP vaccine recipients, while responses from VRP recipients were generally monofunctional and observed in only a few recipients (Figures 6 and 7). The frequency of the response in the VRP-vaccinated animals that did yield multifunctional T cells was somewhat comparable to that in the HPIV3/EboGP recipients (Figures 6 and 7). The functional quality of $CD8^+$ and $CD4^+$ cells from VRP recipients was greater in the spleen, though no discernible pattern in functional marker combinations was observed among the animals (Figure 6). All VRP-vaccinated animals, however, possessed $CD103^+CD8^+$ T cells monofunctional for TNF-α. Blood- and spleen-isolated $CD8^+$ T cells from VRP vaccine recipients exhibited greater response than those isolated from the lungs, with the majority being monofunctional.

Polyfunctional T cells secrete greater amounts of IFN-γ in lungs. We next compared the mean fluorescence intensity (MFI) of IFN-γ for $CD8^+$ and $CD4^+$ T cell populations expressing all IFN-γ–inclusive activation marker combinations. We found that IFN-γ expression by $CD8^+$ T cells gradually increased as the number of functional markers increased, with higher MFI detected in popu-

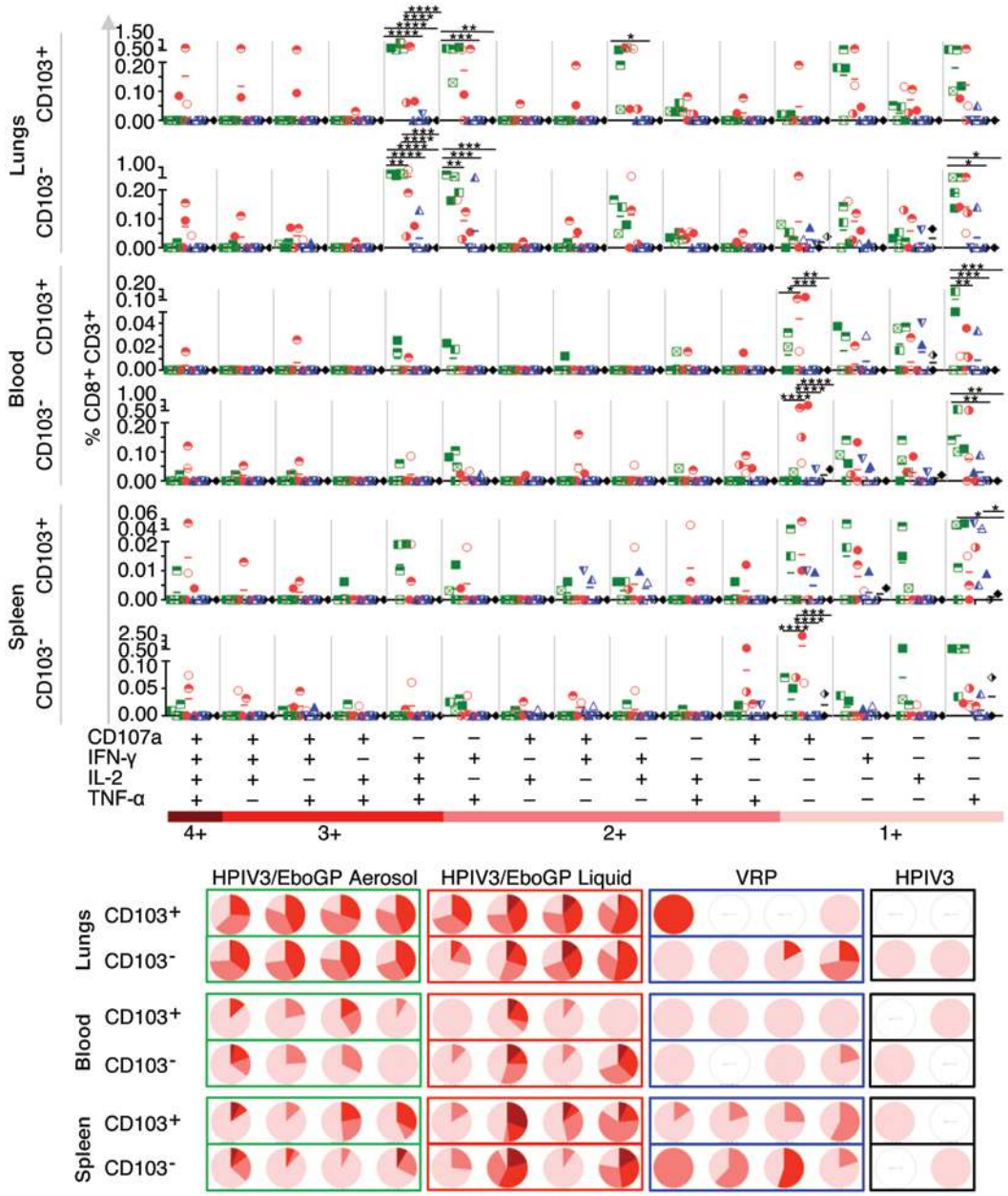

Figure 6. Polyfunctional CD8⁺ T cell response from vaccination study 1. NHPs were vaccinated with aerosol (n = 4; green) or liquid (n = 4; red) HPIV3/EboGP, VRP (n = 4; blue), or HPIV3 control (n = 2; black). Upper panels: percentage of CD103⁺ and CD103⁻ CD8⁺ T cell subsets in the lungs, blood, and spleen of each animal, producing all possible combinations of activation markers. Lower panels: proportion of response patterns for each animal, grouped according to the number of positive markers whereby pie slices represent all 4 (4+, dark red) or any combination of 3 (3+), 2 (2+), or 1 (1+) of the measured markers (the lighter colors). $^{*}P < 0.05$; $^{**}P < 0.01$; $^{***}P < 0.001$; $^{****}P < 0.0001$, by 2-way ANOVA with Tukey's post-hoc test.

lations eliciting all 4 markers of activation, followed by cells positive for 3 markers (IFN-γ⁺TNF-α⁺IL-2⁺), 2 markers (IFN-γ⁺IL-2⁺, IFN-γ⁺TNF-α⁺), and IFN-γ only (Figure 8A). Interestingly, CD8⁺ T cells positive for all 4 markers of activation from the aerosol and liquid HPIV3/EboGP groups produced comparable IFN-γ MFI (Figure 8A) despite the scarcity of these cells in the aerosol group (Figure 6). CD8⁺ T cells from the lungs, blood, and spleen yielded comparable IFN-γ MFI (Figure 8A) despite higher percentages of IFN-γ–positive cells found in the lungs (Figure 5). Similar to the IFN-γ expression trend observed in CD8⁺ T cells, greater IFN-γ MFI were detected in triple-marker CD4⁺ T cell populations positive for IFN-γ, TNF-α, and either IL-4 or IL-17 (Figure 8B) despite their rarity (Figure 7). A high IFN-γ MFI was observed in CD4⁺ T cells coexpressing IFN-γ and TNF-α from the lungs, blood and spleen, while monofunctional cells yielded high IFN-γ MFI only in the lungs of HPV3/EboGP recipients. Taken together, these data suggest that a greater level of activation of cells is accompanied not only by simultaneous secretion of multiple cytokines, but also by the greater level of secretion of IFN-γ by polyfunctional T cells. These data also suggest that respiratory delivery of HPIV3/EboGP induces highly activated T cells in lungs.

Study 2

Protective efficacy of aerosol vaccination. In the second study (Figure 1B), we evaluated protection conferred by aerosolized HPIV3/EboGP administered to rhesus macaques. Due to the high EBOV-neutralizing antibody response induced after the first aerosolized dose (Figure 3A), we included a single-dose group in addition to a 2-dose group. The control groups included animals vaccinated with 2 doses of HPIV3/EboGP delivered to the respiratory tract as a liquid, which were expected to be protected (21), and animals vaccinated with an empty vector. Fol-

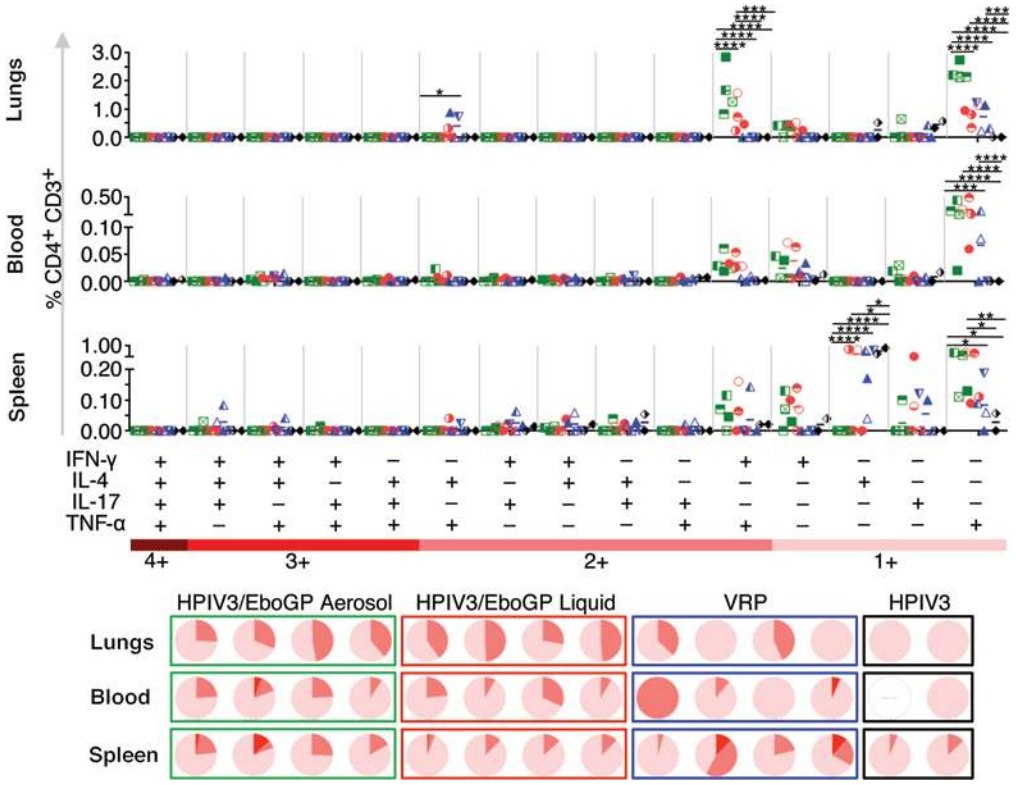

Figure 7. Multiple effector functions of CD4⁺ T cells in study 1 vaccine recipients. CD4⁺ cell response profiles in lungs, blood, and spleen of aerosol (n = 4; green) or liquid (n = 4; red) HPIV3/EboGP, VRP vaccine (n = 4; blue), or HPIV3 control (n = 2; black) recipients from study 1 are shown. The percentage of CD4⁺ T cells eliciting all possible functional response combinations of IFN-γ, IL-4, IL-17, and TNF-α (dot plots) and their proportional contribution (pie charts) to the total EBOV GP–induced response are displayed in the same manner as in Figure 6. $^{*}P < 0.05$; $^{**}P < 0.01$; $^{***}P < 0.001$; $^{****}P < 0.0001$, by 2-way ANOVA with Tukey's post-hoc test.

lowing vaccinations, BAL and serum were periodically collected for analysis of mucosal and systemic antibody responses, respectively. On day 55 (27 days after the second or single vaccination with aerosolized HPIV3/EboGP), the animals were exposed to 1,000 PFU of EBOV delivered by the i.m. route. Following exposure, blood samples were collected every 2 days after infection to analyze viremia and blood chemistry.

Antibody responses to aerosol vaccination. Prior to infection, the 2-dosing schedule of HPIV3/EboGP (aerosol or liquid) resulted in the induction of serum and EBOV-specific mucosal IgG, IgA, and neutralizing titers (Figure 9) in accordance with the humoral response observed in vaccinated rhesus macaques from study 1 (Figure 2). EBOV-specific serum IgG were detected on day 14 after HPIV3/EboGP vaccination (Figure 9A), and levels increased by day 28. After the second dose, antibody levels further increased and plateaued by day 51, the last time point analyzed. IgG levels were similar in animals vaccinated with liquid and aerosolized HPIV3/EboGP. EBOV-specific serum IgA (Figure 9B) was induced with a kinetic pattern similar to that of IgG. The kinetics of IgG and IgA induction were similar between animals administered only a single aerosol HPIV3/EboGP dose and those that received the initial dose of the 2-dose regime. However, at the time of infection, the levels of IgG and IgA in the single-dose group were somewhat lower than in the 2-dose groups. As in study 1 (Figure 3A), high levels of serum EBOV-neutralizing antibodies were detected 28 days after the first dose of HPIV3/EboGP, delivered in either form, which did not increase further following a second dose (Figure 9C). Equal levels of EBOV-neutralizing antibodies were therefore achieved in all groups, including the single-dose aerosol group, at the time of infection.

EBOV-specific mucosal IgG (Figure 9D) and IgA (Figure 9E) were induced after dose 1 (day 21) and marginally increased after dose 2 (day 44), resulting in higher levels in the 2-dose groups compared with the 1-dose aerosol group. In 2-dose groups, mucosal EBOV-neutralizing antibodies were detected after the first dose and were not further augmented by a second dose (Figure 9F). However, in the single-dose aerosol group, mucosal-neutralizing antibodies were detected in only 1 out of the 4 animals despite a robust serum-neutralizing response. This may be explained by inefficient BAL collection or titers below the limit of detection due to the margin between vaccination and BAL collection being 5 fewer days than for animals that received their first inoculation of a 2-dose vaccine regime.

A single dose of aerosolized EBOV/EboGP protects rhesus macaques against EBOV infection. After EBOV infection, the 2 control HPIV3 vector–vaccinated animals demonstrated increased clinical sickness scores. They also demonstrated sharp increases in serum alanine aminotransferase and bilirubin, markers of liver disease, creatinine, marker of kidney disease, and blood urea nitrogen, marker of liver and kidney disease (Figure 10A); all 4 are typically increased during EBOV infections (reviewed in ref. 39). On days 8 and 9 after infection, the animals became moribund and were euthanized (Figure 10B). In contrast, these markers were normal in all HPIV3/EboGP recipients, with the exception of a small transient increase of alanine aminotransferase in 1 recipient of the single aerosol dose on day 10 (Figure 10A). The clinical scores and body temperatures were also normal, with the exception of a small transient increase in an animal vaccinated with 2 doses of aerosolized HPIV3/EboGP, 3 animals vaccinated with 1 dose

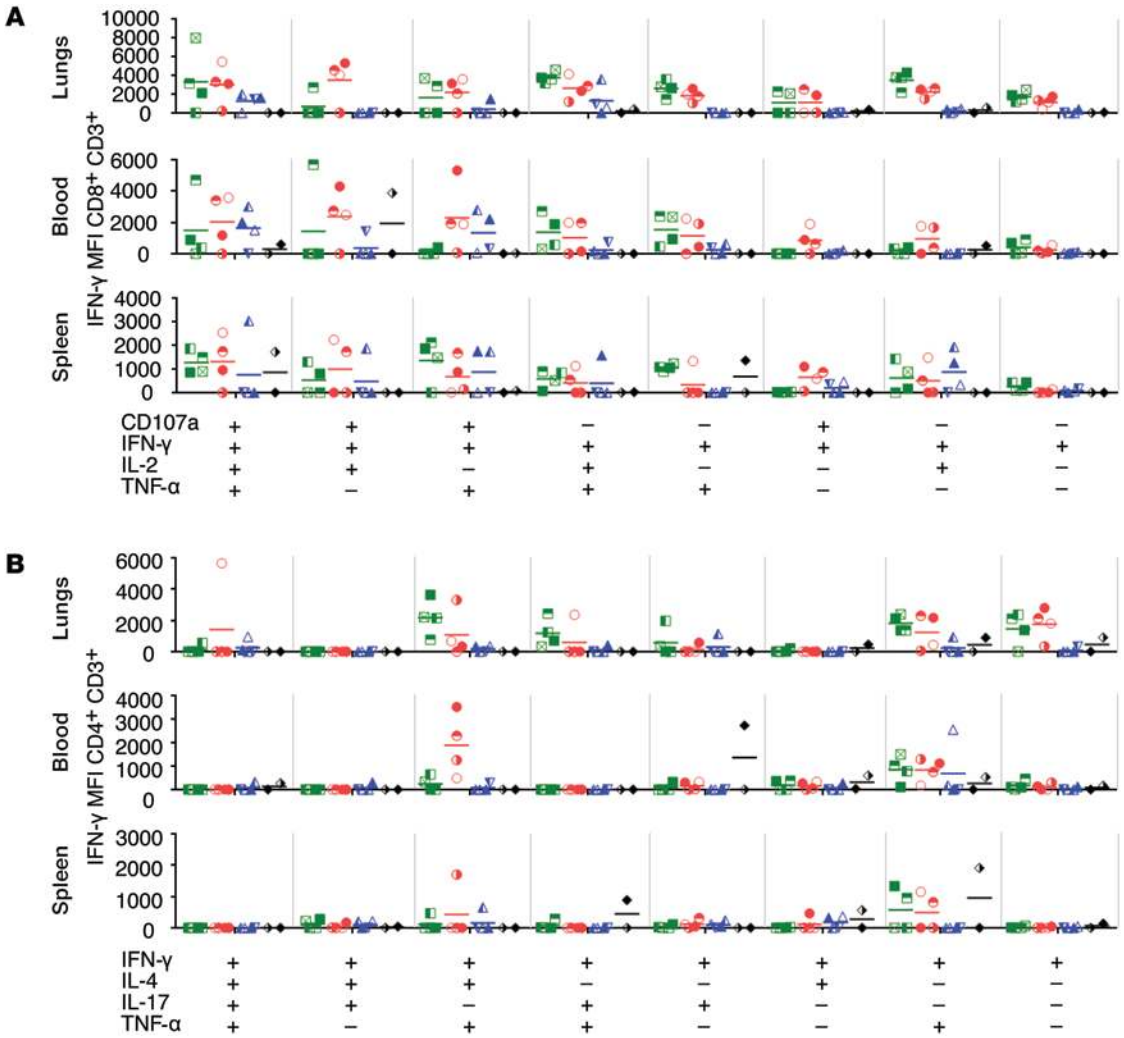

Figure 8. IFN-γ expression in polyfunctional T cells. IFN-γ MFI (*y* axes) for functional response combinations in (**A**) $CD8^+$ and (**B**) $CD4^+$ T cells in the lungs, blood, and spleen of aerosol (n = 4; green) or liquid (n = 4; red) HPIV3/EboGP, the VRP vaccine (n = 4; blue), or HPIV3 control (n = 2; black) recipients from study 1. The *x* axes show combinations of functional markers positive for IFN-γ with CD107a, IL-2, or TNF-α ($CD8^+$) or IL-4, IL-17, or TNF-α ($CD4^+$). IFN-γ MFI for individual animals is shown with horizontal bars representing group means.

of aerosolized HPIV3/EboGP, and 1 animal vaccinated with 2 doses of liquid HPIV3/EboGP (Figure 10, C and D). Plaque titration analysis of serum collected every 2 days after EBOV exposure demonstrated high levels of viremia in the 2 control animals (Figure 10E). In contrast, no viremia was detected in any of the vaccinated animals. Analysis of serum by quantitative real-time reverse-transcription–PCR (RT-PCR), however, demonstrated transient low levels of EBOV RNA in some of the vaccinated animals, which completely disappeared by day 10.

All 10 surviving HPIV3/EboGP-vaccinated animals were euthanized 28 days after infection. H&E and immunohistochemical staining of the spleen, liver, kidney, and lungs of all HPIV3/EboGP-vaccinated, EBOV-infected macaques confirmed normal tissue histology and the absence of EBOV antigen (spleen and liver from a representative HPIV3/EboGP recipient shown in Supplemental Figure 2). Tissues from the control HPIV3 vector–vaccinated macaques displayed EBOV antigen and histologic lesions consistent with EBOV infection, including necrotizing hepatitis and splenic lymphoid depletion (Supplemental Figure 2). Taken together, these data suggest that a single administration of aerosolized HPIV3/EboGP completely protects animals against death and severe disease caused by a uniformly lethal dose of EBOV administered by the i.m. route.

Discussion

In this study, we demonstrate the feasibility of aerosolized delivery of our HPIV3/EboGP vaccine against EBOV in rhesus macaques, which is a practical and noninvasive mode of delivery to the lower respiratory tract. A single dose of aerosolized vaccine achieved uniform protection against lethal infection. Moreover, this study demonstrates, for what we believe is the first time, successful aerosol vaccination against a viral hemorrhagic fever. A single-dose aerosol vaccine would be easily implemented to enable both prevention and containment of EBOV infections in a natural outbreak setting where healthcare infrastructure is deficient or during bioterrorism and biological warfare scenarios.

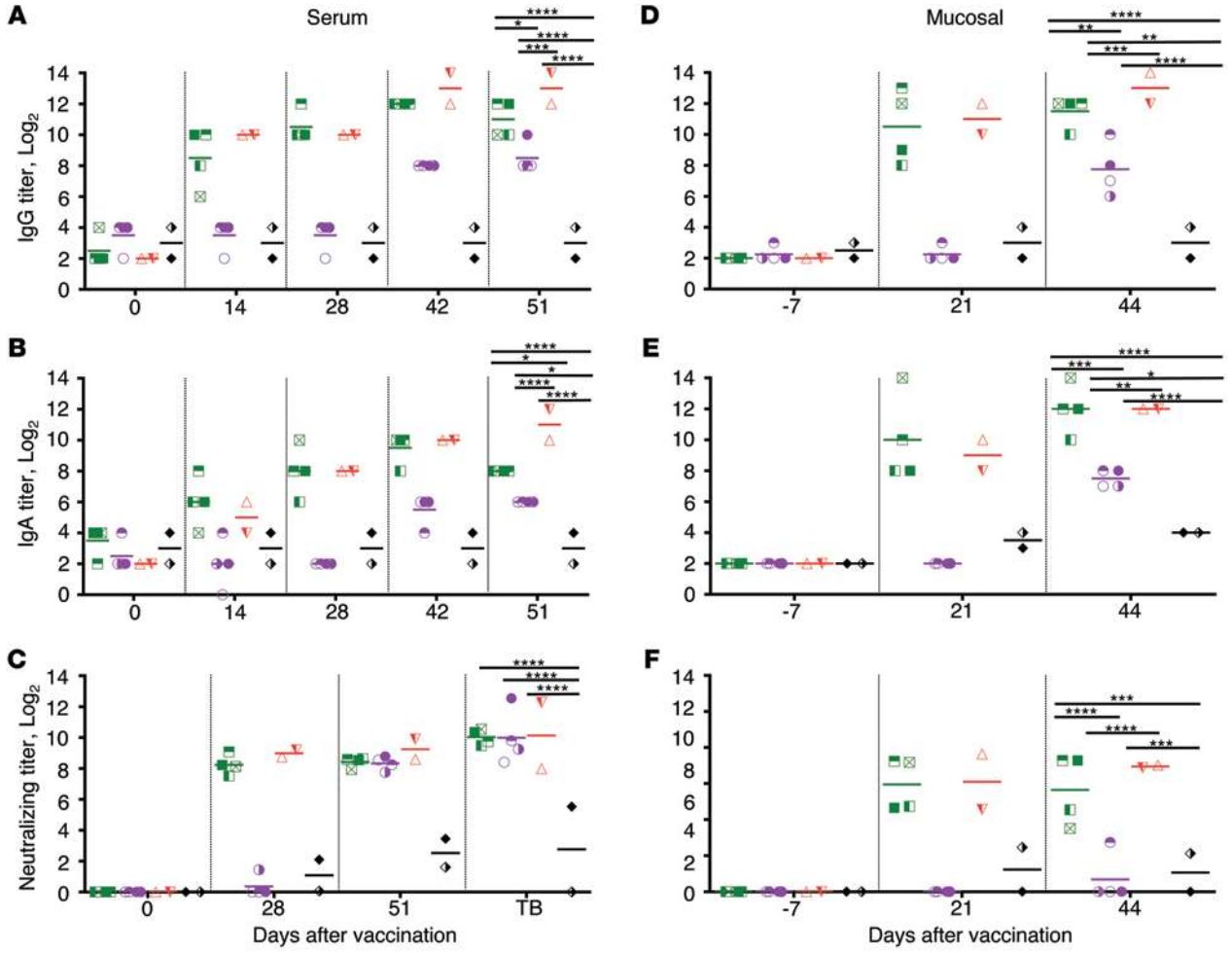

Figure 9. Serum and mucosal antibody responses in EBOV infection study 2. One dose of aerosolized HPIV3/EboGP (n = 4; purple), 2 doses of aerosolized HPIV3/EboGP (n = 4; green), 2 doses of liquid HPIV3/EboGP (n = 2; red), and 2 doses of HPIV3 control (n = 2; black) were given. EBOV-specific IgG and IgA were detected in (**A** and **B**) serum and (**D** and **E**) concentrated BAL fluids by ELISA. EBOV-specific neutralizing antibodies were detected in (**C**) serum and (**F**) mucosa by plaque-reduction assays. TB, terminal bleed. Antibody titers are shown for individual animals in the vaccine groups, with the horizontal bar representing the group means. *P < 0.05; **P < 0.01; ***P < 0.001; ****P < 0.0001, by 2-way ANOVA with Tukey's post-hoc test. For clarity, comparisons made are shown only for the final time point.

To date, studies on cellular immune responses to respiratory viral infections or vaccinations have focused on T cells in circulation, in the BAL fluid, or from small animal models, which can greatly misrepresent the immune dynamics in the respiratory tract. The present study represents what we believe to be the first analysis of the lung-resident T cell response to a respiratory tract vaccine in NHPs. Respiratory vaccination of rhesus macaques with HPIV3/EboGP in either aerosol or liquid form resulted in an induction of EBOV-specific systemic IgG and IgA, which were markedly boosted by the second dose. Remarkably, the high levels of EBOV-neutralizing antibodies generated after the first dose of aerosol and liquid HPIV3/EboGP were comparable and were not further augmented by a second dose, suggesting the possibility of protection by a single liquid vaccine dose. The first dose of HPIV3/EboGP generated greater levels of EBOV-specific antibodies, which possessed better neutralizing and avidity properties than VRP-derived antibodies. After the second dose, the systemic humoral response was comparable between the 2 vaccines. We tested the ability of these antibodies raised against GP of EBOV (isolate Mayinga), which belongs to the species *Zaire ebolavirus*, to cross-neutralize 2 major heterologous species of *ebolavirus*, BDBV and SUDV, whose respective GP amino acid sequences have 66% and 56% similarity to EBOV. Unexpectedly, we detected cross-neutralizing antibodies in some animals vaccinated with either vaccine after dose 1 and in most animals after dose 2 with markedly greater neutralization by antibodies from VRP-vaccinated animals. The greater antibody neutralization of BDBV and SUDV by the VRP vaccine recipients in spite of the reduced neutralization of EBOV when compared with aerosolized HPIV3/EboGP recipients may be attributed to B cell class switching, whose inhibition can skew antibody repertoire away from high-affinity variant epitopes and improve heterotypic protection (40). It is possible that lung B cells are strongly stimulated by HPIV3/EboGP to effectively induce class switching, resulting in a highly potent but narrower antibody response compared with that seen with VRP. Surprisingly, after dose 1, a greater number of animals from all vaccine

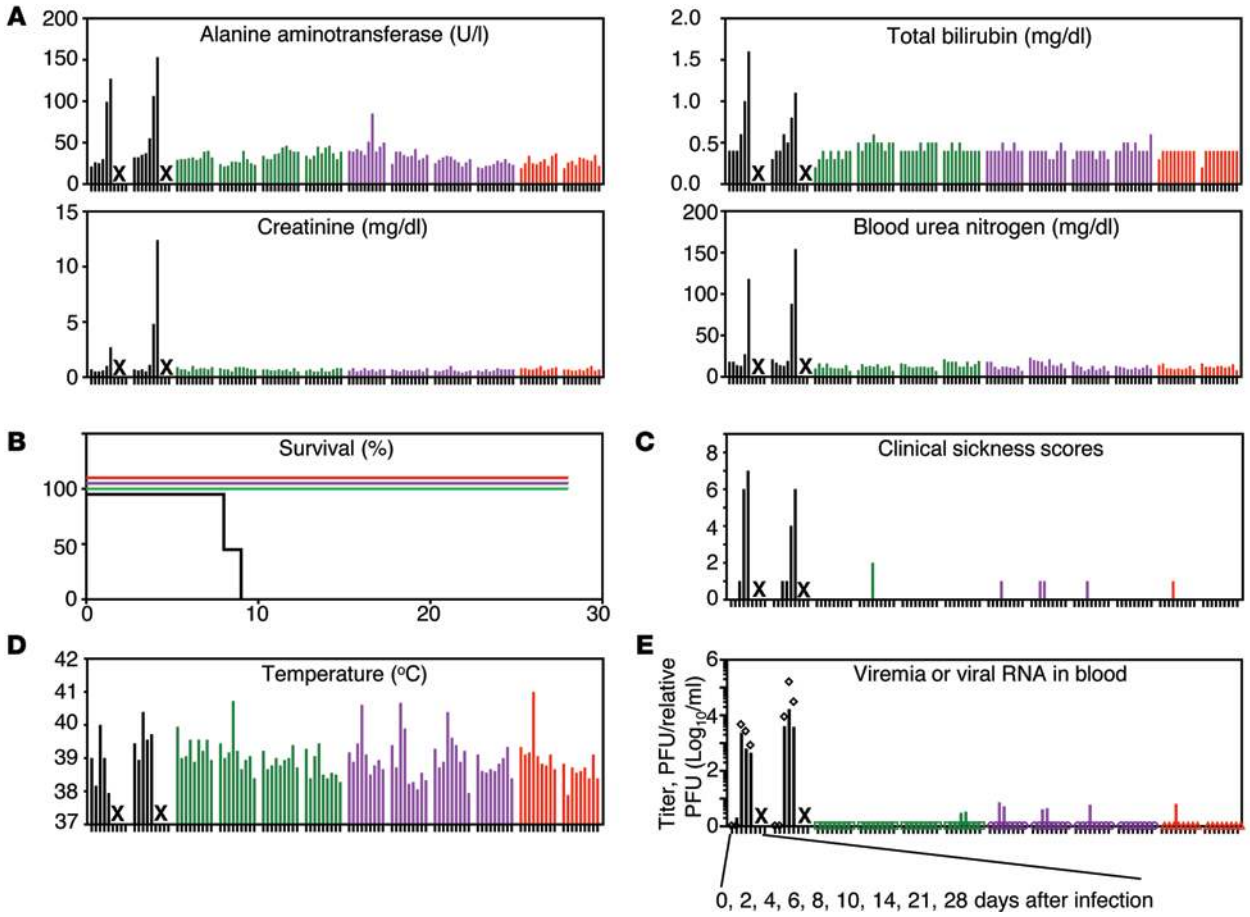

Figure 10. EBOV infection of vaccinated NHPs in study 2. HPIV3 control (*n* = 2; black), 2 doses of HPIV3/EboGP aerosol (*n* = 4; green), 1 dose of HPIV3/EboGP aerosol (*n* = 4; purple), or 2 doses of HPIV3/EboGP liquid (*n* = 2; red) were given. (**A**) Peripheral blood markers of EBOV disease. The values alanine aminotransferase, total bilirubin, creatinine, and blood urea nitrogen are shown for each animal. X's indicates euthanasia of the moribund control animals after the last indicated blood sample was collected. (**B**) Percentage survival over 28 days following i.m. injection of 1,000 PFU of EBOV. (**C**) Clinical sickness scores ranging from 0–9, where 0–3 require no medical intervention and 9 requires euthanasia. (**D**) Temperature. (**E**) Viremia assessed by plaque assay (PFU/ml; symbols) and the levels of viral RNA in serum determined by quantitative RT-PCR (relative PFU/ml; bars). (**A** and **C**–**E**) Values are shown for each animal on days 0, 2, 4, 6, 8,10, 14, 21, and 28 after infection, with the exception of PFU/ml on day 28 (not determined) and relative PFU/ml on days 14, 21, and 28 (not determined).

groups possessed antibodies that were better neutralizers of SUDV than BDBV despite greater overall amino acid similarity between the GP of EBOV and BDBV. This phenomenon may be explained by the presence of certain amino acids in putative protective epitopes of GP, which are conserved between SUDV and EBOV, but not BDBV. For example, amino acids Ser90, Pro116, Gly149, and Asp150, present in the highly conserved receptor-binding domain of GP from EBOV and SUDV, were nonconservatively replaced with Ala, Ala, Glu, and Gly, respectively, in BDBV.

EBOV-specific mucosal IgG, IgA, and neutralizing antibody responses were effectively induced by the first dose of HPIV3/EboGP and markedly boosted by a second dose, resulting in equal levels of antibodies between aerosol and liquid recipients. Given that EBOV is infectious in an aerosolized form (4) or as droplets of respiratory secretions (5) and that its infection route typically involves the mucosa (6, 7, 39), the induction of mucosal antibody responses observed after aerosol vaccination is likely to be an important contribution to the first line of defense against mucosal or respiratory exposure.

The present data demonstrated that HPIV3/EboGP (but not VRP) induces vigorous polyfunctional lung-resident $CD8^+$ and $CD4^+$ T cell responses, which are likely to further enhance mucosal antibody–mediated protection against respiratory tract infection. Following respiratory vaccination with HPIV3/EboGP, the cellular response in lungs, especially from $CD8^+$ T cells, was greater than that in their counterparts in blood and spleen. Greater IFN-γ amounts expressed by these cells indicate they are functionally potent, producing multiple effectors in greater quantities (41). Activated lung-resident $CD8^+$ T cells were predominantly secreting IFN-γ, IL-2, and TNF-α simultaneously, which is indicative of the greatest ability to kill virus-infected cells (42). The activated lung $CD4^+$ T cells had mostly an IFN-γ^+TNF-α^+ or TNF-α^+ phenotype. Aerosol HPIV3/EboGP delivery further enhanced the levels of activated lung $CD4^+$ T cells compared with i.n./i.t. delivery. This may be due to a more effective distribution of the vaccine to pulmonary antigen-presenting cells housed in the bronchiole.

CD103, preferentially expressed by mucosal $CD8^+$ T cells, mediates mucosal tissue tropism and promotes cytolysis through

specific interaction with the E-cadherin ligand on epithelial cells, which triggers lytic granule polarization and exocytosis (31). Respiratory tract $CD8^+$ T cells, but not peripheral blood counterparts with the same antigenic specificity, are highly positive for CD103 and have the effector memory phenotype (43). In human BAL, a much greater fraction of $CD8^+$ and $CD4^+$ T cells expresses CD103, as compared with that in the peripheral blood (31). Analysis of $CD8^+$ T cells demonstrated almost equivalent activation levels among $CD103^+$ and $CD103^-$ subpopulations in the lungs, suggesting that, besides the strong mucosal cell–mediated $CD8^+$ T cell response, respiratory vaccination resulted in the induction of $CD103^-CD8^+$ T cells.

CD107a is a marker of $CD8^+$ T cell degranulation that relocates to the plasma membrane from lytic granules also containing granzyme and perforin (44) to mediate cytolytic activity in an antigen-specific manner (45). Accumulation of CD107a at the cell surface is temporarily linked to downregulation of the lymph node homing marker CD62L, indicating a $CD8^+$ T cell's transition from a central to an effector memory cell (44). Overall, the level of $CD8^+$ T cell degranulation was low in HPIV3/EboGP vaccinees. Mobilizing CD107a populations were also positive for IFN-γ with or without IL-2 and/or TNF-α. As a control measure against damage to the mucosa, lung T cells, in particular $CD103^+CD8^+$ T cells, have a lower cytotoxic potential and a higher expression of CD94/NKG2A, an inhibitory natural killer receptor complex, in comparison with their $CD103^-$ counterparts, but are able to upregulate their effector capacity upon exposure to a specific antigen (46). This may explain why we generally observed lower levels of CD107a in the $CD103^+$ populations as compared with $CD103^-$ T cells. The low expression of CD107a might also be explained by the transient nature of its expression on the surface of the cell, which is followed by its internalization (45).

Studies on experimental filovirus vaccines to date have failed to directly compare the performance of different vaccine platforms, instead relying on published results generated under different conditions to draw comparisons (47). This study provides a side-by-side evaluation of antibody- and cell–mediated responses to 2 very different vaccines: a recombinant paramyxovirus vector administered to the respiratory tract and VRP, administered via the i.m. route. HPIV3/EboGP elicited greater levels of activated $CD8^+$ and $CD4^+$ T cells in lungs and blood, while in the spleen, levels were comparable between the 2 vaccines. Replication of the HPIV3/EboGP vaccine construct in the lungs of guinea pigs is attenuated by 63- to 200-fold compared with the wild-type vector (19, 20), while the level of attenuation in NHPs is unknown. HPIV3/EboGP, whose replication is confined to the respiratory tract (18–20), likely stimulates antigen-presenting cells and induces T cell responses in bronchus-associated lymphoid tissues, as was demonstrated with influenza A virus in mice lacking spleens (48, 49). This results in the retention of the majority of activated T cells in lungs, while some enter systemic circulation and the spleen. In contrast, following the i.m. inoculation of VRP, human dendritic cells are effectively transduced (50) and enter the systemic lymphatic system to activate virus-specific T cells in the spleen and lymph nodes. The overall greater immune response to HPIV3/EboGP is likely related to the fact that, despite its attenuation, it is still capable of effectively attracting antigen-presenting cells such as dendritic cells to the site of the vaccine virus replication to result in effective triggering of the adaptive immune response.

Depending on the type of vaccine, both antibodies (23) and $CD8^+$ T lymphocytes (24) may mediate protection against EBOV exposure. In addition, an emerging body of evidence suggests that $CD4^+$ T cells may also play a role in protection against viral infections due to their direct cytotoxic effect (51). Both the vaccines used in the present study induced systemic EBOV-neutralizing antibody responses, suggesting their role in protection. Moreover, HPIV3/EboGP induced EBOV-specific mucosal antibodies and a prolific $CD8^+$ and $CD4^+$ T lymphocyte response in the lungs. These data indicate that in the case of infection through the i.m. route, protection by both vaccines is likely mediated by antibodies. However, in the case of respiratory mucosal infection, HPIV3/EboGP may induce protection through the induction of both antibody- and cell-mediated responses in the respiratory tract. Furthermore, lung-resident $CD4^+$ T cells are likely to facilitate the induction of systemic antibody responses and therefore indirectly contribute to protection against i.m. exposure. While lung-resident $CD4^+$ T cells cannot be easily quantified in clinical trials, the level of EBOV-neutralizing serum antibody responses is likely to be the best correlate of protection against i.m. exposure.

The demonstration of safety, immunogenicity, and protective efficacy of HPIV3/EboGP in NHPs provides the basis for advancing this experimental vaccine to a phase I clinical study. A clinical study lot of HPIV3/EboGP has been manufactured under the FDA's current good manufacturing practices guidelines using standard cell culture that yields satisfactory titers (above 10^7 PFU/ml) without concentration. Pending regulatory approval through an FDA investigative new drug application, the aerosolized form will be evaluated for replication, safety, and immunogenicity in a dose-escalation study in adults in an inpatient setting. The manufacturer of vaccine for larger studies would be under large-scale optimized growth and purification conditions.

Methods

NHP study 1. A cohort of juvenile male and female rhesus macaques (*Macaca mulatta*; New England Primate Research Center and NIAID Morgan Island Colony, Charles River Laboratories) were used in the vaccination study. On day 0, a group (n = 4) was inoculated via the respiratory tract with 2 ml of HPIV3/EboGP at $10^{8.3}$ PFU/ml (Figure 1A) aerosolized using the Aeroneb Lab nebulizer with a small volume nebulizer unit (Aerogen) that generates particles with a median diameter of 2.5 μM. The nebulizer unit, affixed to a small-sized mask (Rusch) held over the anesthetized animal's nose and mouth, was activated to administer the entire inoculum. Another group (n = 4) received 2 ml of the vaccine at $10^{7.3}$ PFU/ml delivered as a liquid via the combined i.n./i.t. route (0.5 ml per nostril and 1 ml i.t.). The VRP vaccine (10^{10} PFU, 1 ml) was administered to rhesus macaques (n = 4) by i.m. injection. The control group (n = 2) received 2 ml of the HPIV3 empty vector at $10^{7.3}$ PFU/ml via the i.n./i.t. route. On day 28, all animals received a second dose of their respective vaccines. Serum and BAL were sampled over the course of the study. On day 56, animals were euthanized and mononuclear cells were extracted from the lungs, blood, and spleen.

NHP study 2. To determine the protective efficacy of the aerosolized HPIV3/EboGP vaccine, a new cohort of juvenile male and female rhesus macaques (NIAID Morgan Island Colony, Charles River Laboratories) were vaccinated as per study 1 protocol, with the exception that those in one group (n = 4) received only 1 aerosol dose on day 28, 2 rhesus macaques were vaccinated with the liquid form of HPIV3/EboGP, and no animals were vaccinated with the VRP vaccine (Figure 1B). On day 55, all animals were injected by the i.m. route with 1,000 PFU of EBOV (Kikwit, 7U variant; GenBank KC242796.1). Over the course of the study, peripheral blood markers of EBOV disease, measured by VetScan, viremia and viral RNA in serum, and serum and mucosal IgG, IgA, and neutralizing titers were assessed. Animals were monitored for clinical signs of illness and scored 0–9 for each category: dyspnea, depression, recumbency, and rash/hemorrhage. A score of 0–3 required no intervention, while a score of 9 required euthanasia as per IACUC protocol. Surviving animals were euthanized 28 days after infection. Organs were assessed for EBOV antigens and lesions by immunohistochemistry and histopathology, respectively.

Isolation of mononuclear cells. Lungs and spleens were transported in media (RPMI 1640 containing 2 mM L-glutamine, 25 mM HEPES, 100 U/ml penicillin, 100 μg/ml streptomycin, and 10% FBS), weighed, and cut into small 1- to 2-mm cubes for enzymatic digestion in media containing 300 U collagenase type I (Invitrogen) and 100 U type IV bovine pancreatic DNase I (Calbiochem) at 37°C for 90 minutes with gentle shaking. The digest was stopped using 0.01 M EDTA, pH 7.0, filtered through a 250-μM nylon mesh, followed by a 100-μM mesh (BD) to remove particulate matter and washed with an equal volume of cold HBSS. Cells were resuspended in low-density Percoll (P = 1.03 g/ml; GE Healthcare), placed on a high-density Percoll cushion (P = 1.075 g/ml), and centrifuged at 400 g for 20 minutes at 20°C. Cells at the Percoll interface were aspirated and washed twice with HBSS containing 2% FBS. Cells were cryopreserved in 90% FBS containing 10% DMSO until analysis by flow cytometry. Blood was diluted at a 1:1 ratio with PBS, layered onto Ficoll-Paque PLUS (GE Healthcare), and centrifuged at 400 g at 20°C for 30 minutes. Cells at the medium-Ficoll interface were processed under the same conditions as those using the Percoll protocol.

FACS analysis. The frequency of $CD3^+$ T lymphocytes (CD8, CD8 subsets either positive or negative for CD103, and CD4) and their respective markers of activation ($CD8^+$: IFN-γ, TNF-α, IL-2, and CD107a; $CD4^+$: IFN-γ, TNF-α, IL-4, IL-17a) were determined by multiparametric flow cytometry using the following: CD3 Pacific blue (clone SP34-2), CD8 Alexa Fluor 700 (clone RPA-T8), CD4 Alexa Fluor 700 (RPA-T4), CD107a-phycoerythrin (CD107a-PE) (clone H4A3), CD103-FITC (clone HML-1), IL-2–allophycocyanin (IL-2–APC) (clone MQ1-17H12), IL-4–Alexa Fluor 488 (clone 8D4-8), IFN-γ–peridinin chlorophyll (IFN-γ–PerCP) 5.5 (clone 4S.B3), TNF-α PE–cyanine 7 (Cy7) (clone MAb11), and IL-17a PE (clone SCPL1362) (all reagents were obtained from BD Biosciences with the exception of CD103-FITC from Beckman Coulter). Briefly, frozen cells were rested overnight at 2×10^6 cells/ml in culture medium (RPMI containing 25 mM HEPES, 100 U/ml penicillin, 100 U/ml streptomycin, 2 mM L-glutamine and 10% FBS). One million cells were stimulated for 6 hours in culture medium with 10 μg/ml Brefeldin A (Sigma-Aldrich), 0.7 μl/ml GolgiStop (BD Biosciences), 1 μg/ml anti-CD28 (BD Biosciences), 1 μg/ml anti-CD49d (BD Biosciences), and 20 μg/ml DNase (Calbiochem) in the presence of anti-CD107a and either dimethyl sulfoxide or 2.5 μg/ml of 15-mer peptides that overlapped by 11 amino acids and spanned the entire EBOV GP sequence (Mimotopes). After stimulation, cells were washed 2× with wash buffer (PBS, 1% FBS, 0.02% sodium azide) followed by PBS. Cells were stained for surface CD3, CD4, CD8, CD103, and viability (Live/Dead Aqua, Invitrogen) in PBS for 30 minutes at 4°C, washed once with PBS and twice with wash buffer, and permeabilized for 20 minutes at room temperature in Cytofix/Cytoperm (BD Biosciences). Intracellular staining was performed with the relevant antibodies diluted in Perm/Wash buffer (BD Biosciences). Cells were subsequently washed twice with Perm/Wash, followed by PBS. Within 24 hours, 200,000 to 500,000 events were acquired on the BD LSR II Flow Cytometer and data were analyzed using FlowJo version 10 (Tree Star) and SPICE (National Institute of Allergy and Infectious Diseases) software. Background responses were subtracted from responses in peptide-stimulated samples for each marker or response pattern.

Serological assays. For ELISA, sucrose gradient purified, γ-irradiated EBOV (Mayinga isolate) particles were coated onto 96-well Immulux HB plates (Dynex Technologies). Coated plates were blocked with PBS containing 5% nonfat dry milk and 1% BSA (Sigma-Aldrich) for 1 hour at 37°C. Two-fold serial dilutions (starting at 1:4) of serum or BAL concentrated in 30-kDa Vivaspin ultrafiltration spin columns (Sartorius) were applied to the wells and incubated at 37°C for 1 hour. Following 5 washes, bound antibodies were detected with an anti-monkey IgA (KPL; 074-11-011) or IgG (KPL; 074-11-021) HRP conjugate. Following the addition of SureBlue Reserve TMB colorimetric substrate (KPL) and TMB BlueStop solution (KPL), plates were read at 650 nm.

Recombinant EBOV (Mayinga isolate) expressing enhanced GFP (eGFP) (52) (provided by J. Towner and S. Nichol, CDC, Atlanta, Georgia, USA), SUDV variant Gulu (isolate 808892), or BDBV (isolate 811250) stocks for plaque-reduction neutralization assays were generated in Vero-E6 cells and quantified by plaque titrations; 10-fold serially diluted samples were absorbed onto Vero-E6 cells for 1 hour at 37°C and replaced with MEM overlay containing 2% FBS and 0.9% methylcellulose (Sigma-Aldrich). On days 3 to 4, monolayers were fixed with formalin and plaques were visualized under a UV microscope in the case of EBOV-eGFP or immunostained. Briefly, plates were blocked with PBS containing 5% nonfat dry milk for 1 hour at 37°C, followed by the addition of mouse polyclonal antibodies specific for EBOV generated by s.c. inoculation with mouse-adapted EBOV (Mayinga isolate) (provided by Thomas Ksiazek, University of Texas Medical Branch) diluted 1:1,000 in blocking buffer. Bound antibody was detected using secondary goat anti-mouse HRP conjugate (1:2,000 dilution, KPL; 074-1806) and the 4CN Peroxidase Colorimetric Substrate System (KPL). For plaque-reduction neutralization assays, 2-fold serial dilutions of heat-inactivated serum or concentrated BAL at an initial dilution of 1:10 and 1:5, respectively, were prepared in MEM supplemented with guinea pig complement and incubated with virus for 1 hour at 37°C at a final concentration of 100 PFU and 5% complement. Virus-serum mixtures then were absorbed onto Vero-E6 monolayers for 1 hour at 37°C and replaced with MEM overlay. Plaques were detected as described above. Neutralization titer was determined with an end point of 60% plaque reduction.

Steady-state equilibrium and off-rate binding of sera were analyzed by SPR using the Biacore T100. Inactivated sucrose gradient–purified EBOV particles were immobilized at 5,000 RU on a CM5 sensor chip (GE Healthcare) by amine coupling. Serum, diluted 10-fold in 1× HBS-P$^+$ buffer (GE Healthcare) and 10% NSB Reducer (GE Healthcare), was injected sequentially at a flow rate of 30 μl/min. Association and dissociation were performed over 600-second intervals. Antibody off-rates describing the stability of the complex that decays per second were determined from serum sample interaction with the particle, as described above, with the exception that contact time for association was 120 seconds. Rates were calculated using the Biacore software dissociation model. Dissociation rates were independent of total EBOV-antibody binding as determined by injecting both 10- and 100-fold dilutions of serum.

Viremia and viral RNA in blood. Viremia in serum was determined by plaque titrations as described above. EBOV genomic RNA in serum was measured by real-time TaqMan quantitative RT-PCR. RNA was extracted with the QIAamp Viral RNA Extraction Kit (QIAGEN) using Buffer AVL (QIAGEN) at a serum to buffer volume ratio of 1:6. First-strand cDNA synthesis was performed with a sense-strand, nucleoprotein gene-specific primer and Superscript III Reverse Transcriptase (Invitrogen). Real-time RT-PCR was performed with the ABI 7900HT system, and primers and probes specific for the nucleoprotein gene were conserved among EBOV (GenBank NC002549): forward TTTTCAAGAGAGTGCGGACAGTT, reverse CTCCCTGGTACGCATGATGA; probe CCTTCTCATGCTTTGTC-FAM (Invitrogen). Absolute quantification was achieved using a standard curve generated by serial dilution of a virus stock template with known PFU/ml to produce relative PFU values for serum samples.

Histopathology and immunohistochemistry. Tissues fixed in neutral buffered formalin and embedded in paraffin were cut into 5-μm sections and mounted onto slides for immunohistochemistry or H&E staining. For immunohistochemistry, antigen was retrieved with 10 mM sodium citrate, pH 6.0, for 20 minutes at 98°C followed by cooling for 20 minutes at room temperature. Slides were then treated with 3% hydrogen peroxide for 10 minutes and rinsed in running deionized water for 10 minutes. Sections were blocked using the Avidin/Biotin Blocking Kit (Invitrogen) and washed in TBS (Thermo Scientific). An EBOV-specific mouse-polyclonal antibody (provided by Thomas Ksiazek) diluted 1:1,600 in Dako antibody diluent was applied for 1 hour, then washed with TBS. Bound antibody was detected with biotinylated secondary goat anti-mouse IgG (1:200 dilution; Vector Laboratories; catalog BA-9200) and prediluted streptavidin-HRP (Dako). Slides were developed with 3,3′-diaminobenzidine chromogen (Dako) and counterstained in hematoxylin (Harris).

Statistics. Statistical significance was calculated using 2-way ANOVA, Tukey's multiple comparison test, and multiple unpaired, 2-tailed *t* test with Holm-Sidak correction (GraphPad Prism software version 6). A *P* value of less than 0.05 was considered significant.

Study approval. Vaccination procedures for both studies were conducted at the NIH Animal Center (Poolesville, Maryland, USA) and were approved by the NIH Animal Care and Use Committee. The EBOV infection was performed in BSL-4 biocontainment at the Galveston National Laboratory, University of Texas Medical Branch, and infection procedures were approved by the University of Texas Medical Branch Animal Care and Use Committee.

Acknowledgments

We thank Richard Herbert and the staff at the NIH Animal Center for their assistance with the NHP vaccinations. We are indebted to Lijuan Yang and other members of the RNA Viruses Section, Laboratory of Infectious Diseases, National Institute of Allergy and Infectious Diseases, NIH, for helping with extraction of mononuclear cells from organs of NHPs. We also thank Joan Geisbert, Jessica Graber, and the Animal Resources Center of the Galveston National Laboratory for assisting with EBOV infection of NHPs. We thank Luis Holthauzen and the Sealy Center for Structural Biology and Molecular Biophysics of the University of Texas Medical Branch at Galveston for providing valuable support and access to the Biacore T100. This work was supported by the National Institute of Allergy and Infectious Diseases, NIH Western Regional Center of Excellence for Biodefense and Emerging Infectious Diseases (WRCE), grant 5U54AI057156-10, Developmental Project DP007 (to A. Bukreyev); the National Institute of Allergy and Infectious Diseases, NIH, grant 1R01AI102887-01A1 (to A. Bukreyev); and the National Institute of Allergy and Infectious Diseases, NIH Intramural Program (to P.L. Collins).

Address correspondence to: Alexander Bukreyev, Departments of Pathology and Microbiology and Immunology, Galveston National Laboratory, Keiller Building, Room 3.145, University of Texas Medical Branch, 301 University Boulevard, Galveston, Texas 77555-0609, USA. Phone: 409.772.2829; E-mail: alexander.bukreyev@utmb.edu.

1. CDC. Outbreaks Chronology: Ebola Virus Disease. CDC Web site. http://www.cdc.gov/vhf/ebola/outbreaks/history/chronology.html. Updated June 8, 2015. Accessed June 8, 2015.
2. CDC. 2014 Ebola Outbreak in West Africa — Case Counts. CDC Web site. http://www.cdc.gov/vhf/ebola/outbreaks/2014-west-africa/case-counts.html. Updated June 8, 2015. Accessed June 8, 2015.
3. Feldmann H, Sanchez A, Geisbert TW. *Filoviridae: Marburg and Ebola Viruses*. Philadelphia, Pennsylvania, USA: Lippincott Williams & Wilkins; 2013.
4. Johnson E, Jaax N, White J, Jahrling P. Lethal experimental infections of rhesus monkeys by aerosolized Ebola virus. *Int J Exp Pathol*. 1995;76(4):227–236.
5. Jaax N, et al. Transmission of Ebola virus (Zaire strain) to uninfected control monkeys in a biocontainment laboratory. *Lancet*. 1995;346(8991–8992):1669–1671.
6. Jaax NK, et al. Lethal experimental infection of rhesus monkeys with Ebola-Zaire (Mayinga) virus by the oral and conjunctival route of exposure. *Arch Pathol Lab Med*. 1996;120(2):140–155.
7. Wong G, et al. Ebola virus transmission in Guinea pigs. *J Virol*. 2015;89(2):1314–1323.
8. Osterholm MT, et al. Transmission of Ebola viruses: what we know and what we do not know. *MBio*. 2015;6(2):e00137.
9. Halle S, et al. Induced bronchus-associated lymphoid tissue serves as a general priming site for T cells and is maintained by dendritic cells. *J Exp Med*. 2009;206(12):2593–2601.
10. Varol C, et al. Monocytes give rise to mucosal, but not splenic, conventional dendritic cells. *J Exp Med*. 2007;204(1):171–180.
11. de Bree GJ, van Leeuwen EM, Out TA, Jansen HM, Jonkers RE, van Lier RA. Selective accumulation of differentiated CD8$^+$ T cells specific for respiratory viruses in the human lung. *J Exp Med*. 2005;202(10):1433–1442.
12. Hufford MM, Kim TS, Sun J, Braciale TJ. Antiviral CD8$^+$ T cell effector activities in situ are regulated by target cell type. *J Exp Med*. 2011;208(1):167–180.
13. DiNapoli JM, et al. Immunization of primates with a Newcastle disease virus-vectored vaccine via the respiratory tract induces a high titer of serum neutralizing antibodies against

highly pathogenic avian influenza virus. *J Virol*. 2007;81(21):11560–11568.
14. Morokutti A, Muster T, Ferko B. Intranasal vaccination with a replication-deficient influenza virus induces heterosubtypic neutralising mucosal IgA antibodies in humans. *Vaccine*. 2014;32(17):1897–1900.
15. Carter NJ, Curran MP. Live attenuated influenza vaccine (FluMist(R); Fluenz): a review of its use in the prevention of seasonal influenza in children and adults. *Drugs*. 2011;71(12):1591–1622.
16. Farrar JD, Smith JD, Murphy TL, Leung S, Stark GR, Murphy KM. Selective loss of type I interferon-induced STAT4 activation caused by a minisatellite insertion in mouse Stat2. *Nat Immunol*. 2000;1(1):65–69.
17. Rogge L, et al. The role of Stat4 in species-specific regulation of Th cell development by type I IFNs. *J Immunol*. 1998;161(12):6567–6574.
18. Bukreyev A, et al. A single intranasal inoculation with a paramyxovirus-vectored vaccine protects guinea pigs against a lethal-dose Ebola virus challenge. *J Virol*. 2006;80(5):2267–2279.
19. Yang L, Sanchez A, Ward JM, Murphy BR, Collins PL, Bukreyev A. A paramyxovirus-vectored intranasal vaccine against Ebola virus is immunogenic in vector-immune animals. *Virology*. 2008;377(2):255–264.
20. Bukreyev A, et al. Chimeric human parainfluenza virus bearing the Ebola virus glycoprotein as the sole surface protein is immunogenic and highly protective against Ebola virus challenge. *Virology*. 2009;383(2):348–361.
21. Bukreyev A, et al. Successful topical respiratory tract immunization of primates against Ebola virus. *J Virol*. 2007;81(12):6379–6388.
22. Borio L, et al. Hemorrhagic fever viruses as biological weapons: medical and public health management. *Jama*. 2002;287(18):2391–2405.
23. Marzi A, et al. Antibodies are necessary for rVSV/ZEBOV-GP-mediated protection against lethal Ebola virus challenge in nonhuman primates. *Proc Natl Acad Sci U S A*. 2013;110(5):1893–1898.
24. Sullivan NJ, et al. CD8$^+$ cellular immunity mediates rAd5 vaccine protection against Ebola virus infection of nonhuman primates. *Nat Med*. 2011;17(9):1128–1131.
25. Pushko P, et al. Recombinant RNA replicons derived from attenuated Venezuelan equine encephalitis virus protect guinea pigs and mice from Ebola hemorrhagic fever virus. *Vaccine*. 2000;19(1):142–153.
26. Lu D, Hickey AJ. Pulmonary vaccine delivery. *Expert Rev Vaccines*. 2007;6(2):213–226.
27. Cheng YS, Irshad H, Kuehl P, Holmes TD, Sherwood R, Hobbs CH. Lung deposition of droplet aerosols in monkeys. *Inhal Toxicol*. 2008;20(11):1029–1036.
28. Corbett M, et al. Aerosol immunization with NYVAC and MVA vectored vaccines is safe, simple, and immunogenic. *Proc Natl Acad Sci U S A*. 2008;105(6):2046–2051.
29. Olinger GG, Hart MK. Filoviruses: Recent advances and future challenges. Protective Immunity to Ebola Infection by Venezuelan Equine Encephalitis Virus Replicons Expressing Ebola Virus Proteins. Presented at: An ICID Global Symposium; Winnipeg, Manitoba, Canada: 2006.
30. Herbert AS, et al. Venezuelan equine encephalitis virus replicon particle vaccine protects nonhuman primates from intramuscular and aerosol challenge with ebolavirus. *J Virol*. 2013;87(9):4952–4964.
31. Le Floc'h A, et al. αEβ7 integrin interaction with E-cadherin promotes antitumor CTL activity by triggering lytic granule polarization and exocytosis. *J Exp Med*. 2007;204(3):559–570.
32. Kohyama S, et al. IL-23 enhances host defense against vaccinia virus infection via a mechanism partly involving IL-17. *J Immunol*. 2007;179(6):3917–3925.
33. McKinstry KK, et al. IL-10 deficiency unleashes an influenza-specific Th17 response and enhances survival against high-dose challenge. *J Immunol*. 2009;182(12):7353–7363.
34. Chioato A, Noseda E, Stevens M, Gaitatzis N, Kleinschmidt A, Picaud H. Treatment with the interleukin-17A-blocking antibody secukinumab does not interfere with the efficacy of influenza and meningococcal vaccinations in healthy subjects: results of an open-label, parallel-group, randomized single-center study. *Clin Vaccine Immunol*. 2012;19(10):1597–1602.
35. Hou W, Kang HS, Kim BS. Th17 cells enhance viral persistence and inhibit T cell cytotoxicity in a model of chronic virus infection. *J Exp Med*. 2009;206(2):313–328.
36. McAleer JP, Kolls JK. Directing traffic: IL-17 and IL-22 coordinate pulmonary immune defense. *Immunol Rev*. 2014;260(1):129–144.
37. Chang SH, et al. T helper 17 cells play a critical pathogenic role in lung cancer. *Proc Natl Acad Sci U S A*. 2014;111(15):5664–5669.
38. Annunziato F, et al. Phenotypic and functional features of human Th17 cells. *J Exp Med*. 2007;204(8):1849–1861.
39. Kuhn JH. *Filoviruses*. Wien, New York, USA: Springer; 2008.
40. Keating R, et al. The kinase mTOR modulates the antibody response to provide cross-protective immunity to lethal infection with influenza virus. *Nat Immunol*. 2013;14(12):1266–1276.
41. Seder RA, Darrah PA, Roederer M. T-cell quality in memory and protection: implications for vaccine design. *Nat Rev Immunol*. 2008;8(4):247–258.
42. Almeida JR, et al. Superior control of HIV-1 replication by CD8$^+$ T cells is reflected by their avidity, polyfunctionality, and clonal turnover. *J Exp Med*. 2007;204(10):2473–2485.
43. Woodberry T, et al. αEβ7 (CD103) expression identifies a highly active, tonsil-resident effector-memory CTL population. *J Immunol*. 2005;175(7):4355–4362.
44. Wolint P, Betts MR, Koup RA, Oxenius A. Immediate cytotoxicity but not degranulation distinguishes effector and memory subsets of CD8$^+$ T cells. *J Exp Med*. 2004;199(7):925–936.
45. Betts MR, et al. Sensitive and viable identification of antigen-specific CD8$^+$ T cells by a flow cytometric assay for degranulation. *J Immunol Methods*. 2003;281(1–2):65–78.
46. Piet B, et al. CD8(+) T cells with an intraepithelial phenotype upregulate cytotoxic function upon influenza infection in human lung. *J Clin Invest*. 2011;121(6):2254–2263.
47. Richardson JS, Dekker JD, Croyle MA, Kobinger GP. Recent advances in Ebolavirus vaccine development. *Hum Vaccin*. 2010;6(6):439–449.
48. Moyron-Quiroz JE, et al. Role of inducible bronchus associated lymphoid tissue (iBALT) in respiratory immunity. *Nat Med*. 2004;10(9):927–934.
49. Moyron-Quiroz JE, et al. Persistence and responsiveness of immunologic memory in the absence of secondary lymphoid organs. *Immunity*. 2006;25(4):643–654.
50. Moran TP, Collier M, McKinnon KP, Davis NL, Johnston RE, Serody JS. A novel viral system for generating antigen-specific T cells. *J Immunol*. 2005;175(5):3431–3438.
51. Sant AJ, McMichael A. Revealing the role of CD4$^+$ T cells in viral immunity. *J Exp Med*. 2012;209(8):1391–1395.
52. Towner JS, et al. Generation of eGFP expressing recombinant Zaire ebolavirus for analysis of early pathogenesis events and high-throughput antiviral drug screening. *Virology*. 2005;332(1):20–27.